

PAPER • OPEN ACCESS

Heat and mass transfer analysis of MHD peristaltic flow through a compliant porous channel with variable thermal conductivity



To cite this article: H Vaidya *et al* 2020 *Phys. Scr.* **95** 045219

View the [article online](#) for updates and enhancements.

You may also like

- [Thermophoretic particles deposition in time-dependent magneto flow over oscillatory spinning disk](#)
A Rauf, S A Shehzad, T Mushtaq et al.
- [Numerical simulation for homogeneous–heterogeneous reactions and Newtonian heating in the silver-water nanofluid flow past a nonlinear stretched cylinder](#)
Muhammad Suleman, Muhammad Ramzan, Shafiq Ahmad et al.
- [Micropolar fluid past a convectively heated surface embedded with nth order chemical reaction and heat source/sink](#)
Tanveer Sajid, Wasim Jamshed, Faisal Shahzad et al.

Heat and mass transfer analysis of MHD peristaltic flow through a compliant porous channel with variable thermal conductivity

H Vaidya¹ , C Rajashekhar^{2,5} , G Manjunatha², K V Prasad¹,
O D Makinde³ and K Vajravelu⁴

¹ Department of Mathematics, VSK University, Vinayaka Nagar, Ballari-583 105, Karnataka, India

² Department of Mathematics, Manipal Institute of Technology, Manipal Academy of Higher Education, Manipal, Karnataka, 576104, India

³ Faculty of Military Science, Stellenbosch University, Private Bag X2, Saldanha 7395, South Africa

⁴ Department of Mathematics, University of Central Florida, Orlando, FL 32816, United States of America

E-mail: choudhariraj3@gmail.com

Received 5 October 2019, revised 24 December 2019

Accepted for publication 6 January 2020

Published 18 February 2020



CrossMark

Abstract

The MHD peristaltic motion of Bingham fluid through a uniform channel is examined under the influence of long wavelength and small Reynolds number. The impact of variable thermal conductivity, convective heat transfer, porous boundaries, and wall properties are considered. The semi-analytical technique is utilized to solve the governing nonlinear temperature equation. The effects of different parameters on the physiological quantities of interest are captured with the assistance of MATLAB programming. The assessment reveals that an ascent in a magnetic parameter reduces the velocity field. Further, an increment in the estimation of variable thermal conductivity upgrades the temperature profiles. Besides, the trapped bolus is a function of a porous parameter, and an increase in porous parameter will have the proportional increment in the other parameter.

Keywords: Darcy number, concentration slip, wall rigidity, magnetic parameter, viscous damping force parameter

(Some figures may appear in colour only in the online journal)

Nomenclature

x, y	axial and radial co-ordinates	n_2	coefficient of wall damping force
u, v	axial and radial velocities	Da	Darcy number (porous parameter)
Bi	Biot number	Ec	Eckert number
Br	Brinkman number	$\tau_{xx}, \tau_{xy}, \tau_{yy}$	extra stress components
D_m	coefficient of mass diffusivity	B_0	magnetic field strength
		M	magnetic parameter (Hartmann number)
		E_2	mass characterization parameter
		n_1	mass per unit area
		T_m	mean fluid temperature
		Pr	Prandtl number
		p	pressure
		P	pressure gradient

⁵ Author to whom any correspondence should be addressed.



Original content from this work may be used under the terms of the [Creative Commons Attribution 4.0 licence](https://creativecommons.org/licenses/by/4.0/). Any further distribution of this work must maintain attribution to the author(s) and the title of the work, journal citation and DOI.

a	radius of the channel
Re	Reynolds number
n_3	rigidity of the plate
E_4	rigidity parameter
Sc	Schmidt number
Sr	Soret number
c_p	specific heat at constant volume
H	spring stiffness
k	thermal conductivity
K_T	thermal diffusion ration
t	time
E_3	wall damping parameter
E_5	wall elastic parameter
E_1	wall tension parameter
b	wave amplitude
c	wave speed

Greek Letters

ε	amplitude ratio
ϕ	coefficient of thermal conductivity
σ	concentration
γ	concentration slip parameter
ρ	density
σ_1	electric conductivity
ψ	streamline
θ	temperature
α	velocity slip parameter
μ	viscosity
λ	wavelength

1. Introduction

The mechanism of peristaltic motion is well known to the research community from the last few decades because of its significant application in the fields of medicine and industry. This mechanism plays an essential role in understanding the mechanisms involved in food transport through the esophagus, chyme movement in the gastrointestinal tract, urine flow through the ureter, and the flow of blood in vessels. Apart from the biological applications, the peristaltic mechanism is used in designing heart-lung and dialysis machines. The peristaltic mechanism was initiated by Latham [1] for analyzing the flow of urine through ureter. Since then, several scientists have examined peristaltic flow through multiple geometric forms with distinct non-Newtonian fluids [2–5]. In recent decade research has become humble among many scientists in the areas of the building, oil, forestry, mechanical, and chemical engineering in peristalsis, which flow through porous structures. Some of these applications include

transport of contaminants in aquifers, heat and mass transport in chemical engineering, filtration and biomechanical investigation of biological fluids flowing through lungs, blood vessels, and other organs. El-Shehawey *et al* [6] launched the study on the peristaltic system passing through a porous medium. The peristaltic stream of non-Newtonian fluid in the inclined channel was evaluated later by Khan *et al* [7]. Examinations on peristaltic transport through porous media have recently been recorded in the literature [8–10].

In the lack of heat transfer, most of the above examinations on peristaltic flow were performed. However, because of their extensive implementation in the sector of medicine, heat transfer in biological systems is of utmost significance. Three distinct methods, such as convection, conduction, and radiation, can be used for heat transfer in bio-systems. The convective technique plays an essential role in understanding blood oxygenation and hemodialysis among the three modes of heat transfer. Besides, human lungs, gallbladder stones, small-radius blood vessels, etc function as usual porous media, making it essential to offer owing significance to porous media. Also, liquids showing variable thermal conductivity can best approximate the blood passing through arteries. Several scientists [11, 12] conducted the inquiries on this front. Mass transfer is another significant event in knowing the spread of nutrients from the blood to its surrounding tissues. Mass transition performs an essential part in recognizing the procedures engaged in inverse osmosis, cell segregation, chemical impurity propagation, and distillation method in most manufacturing applications. Driven by heat and mass transfer applications, several scientists have researched the impact of these parameters in various geometrical configurations [13–22].

The peristaltic movement of physiological liquids by taking the MHD effect is crucial for physiology and biology. Due to the development of conducting fluid over the magnetic field, electrical flow is prompted. Due to mechanical forces emerging as a result of the magnetic field on these currents, the fluid stream is altered. The operation of MHD blowers, blood siphon machines, heat exchanger structure, stream meters, control generators, radar frameworks, and so on depends on MHD principles. These principles have been used for target drug transport in the medical science, blood flow controls during surgery, cells separation magnetic gadgets, magnetic tracer advances, hyperthermia, and so forth. The therapy of Magneto primarily involves non-Newtonian MHD. The motion of the urine stream through the ureter, the changes in cells and the tissues and blood flow in the arteries is particularly crucial with peristaltic MHD conditions. Motivated by the applications of MHD flows, various researchers have analyzed the impact of MHD peristaltic flow through different geometries [23–28].

Due to their application in the field of health sciences, various specialists have noted the effects of wall properties, such as wall rigidity, viscous damping force, wall stiffness, wall tension, and elastic parameters attracted attention from early on. Hayat *et al* [29] studied the impact of MHD Jeffery fluid through a porous channel. Srinivas *et al* [30] analyzed the effect of wall properties along with slip conditions on the

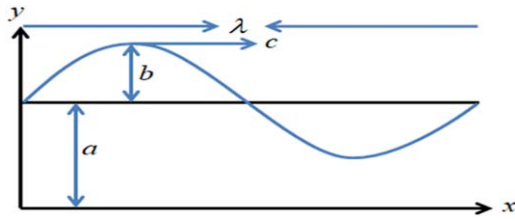


Figure 1. Geometry of the problem.

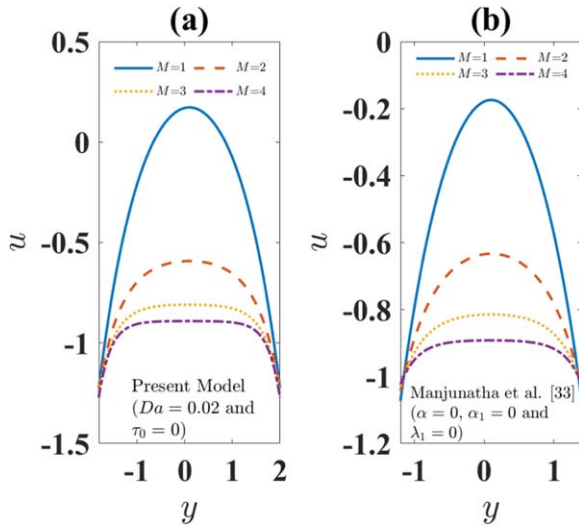


Figure 2. Validation of the model.

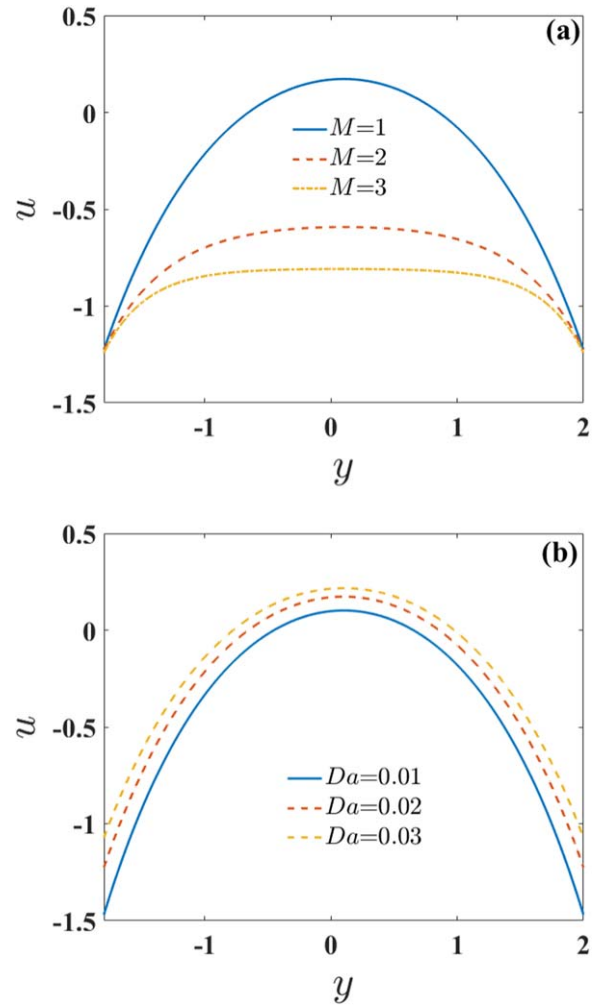


Figure 3. u versus y for varying (a) M and (b) Da .

peristaltic flow. Subsequently, the impact of wall properties on peristalsis by using Burgers fluid was researched by Javed *et al* [31]. The effects of wall properties on peristaltic transport of Rabinowitsch fluid by porous channels were investigated by Vaidya *et al* [32]. Recently, Manjunatha *et al* [33] analyzed the impact of variable viscosity and variable thermal conductivity on the MHD peristaltic flow of Jeffrey fluid. Most biofluids have non-Newtonian behavior. According to the area of its flow, the blood has a dual nature. Generally, it behaves Newtonian when it is flowing through the large arteries where there exists a linear relationship between stress and strain. However, non-Newtonian behavior is noticed when the flow is associated with micro arteries. Due to the complex action of blood, it is difficult to describe the various rheological effects such as hematocrit, shear rate, variable viscosity, etc. Thus, many approaches exist to define these equations, some of them as a result of fitting a curve to an experimental data and others based on some rheological models. Among the multiple non-Newtonian models, the Bingham model has lately been used in literature to study the peristaltic system through various geometries [34–36].

This study aims to build on the work of the researchers, as previously mentioned, in the presence of heat and mass transfer of the MHD peristaltic mechanism for Bingham fluid. Moreover, the effects of convective and wall properties are considered. Since very few papers have considered the variable thermal conductivity in their formulation, this article seeks, by examining the fluid to exhibit these properties, to

bridge the gap in its formulation. The writers attempted to create a mathematical model that would provide realistic demonstrations of blood flow.

2. Mathematical formulation of the problem

Consider a viscous fluid that flows through a uniform channel of radius a (see figure 1). The fluid is controlled by non-Newtonian Bingham liquid caused by sinusoidal wave trains of wavelength λ . For simplicity, the channel is assumed to be axisymmetric. The channel is horizontal, with its walls being flexible because of wall properties. Further, the flow is exposed to an external magnetic field of strength B_0 , which is applied in the direction perpendicular to the fluid flow. The electric field is taken to be zero. Also, the magnetic Reynolds number is assumed to be very small so that the induced magnetic field is negligible in comparison to the external magnetic field. The variable thermal conductivity of the non-Newtonian Bingham model is considered in the analysis. The porous conditions, convective conditions, and concentration slip are considered. The sinusoidal wave that travels along the

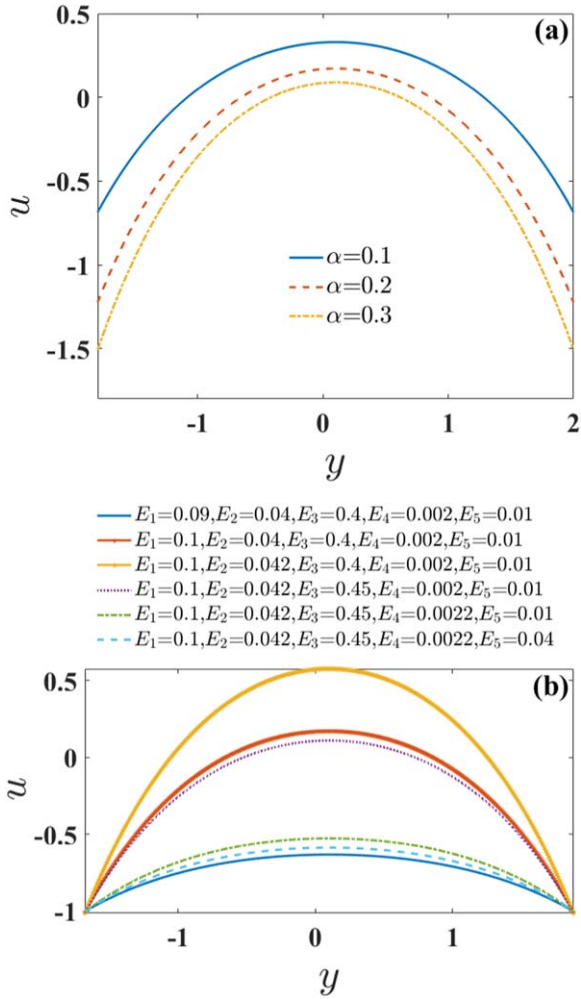


Figure 4. u versus y for varying (a) α and (b) $E_1 - E_5$.

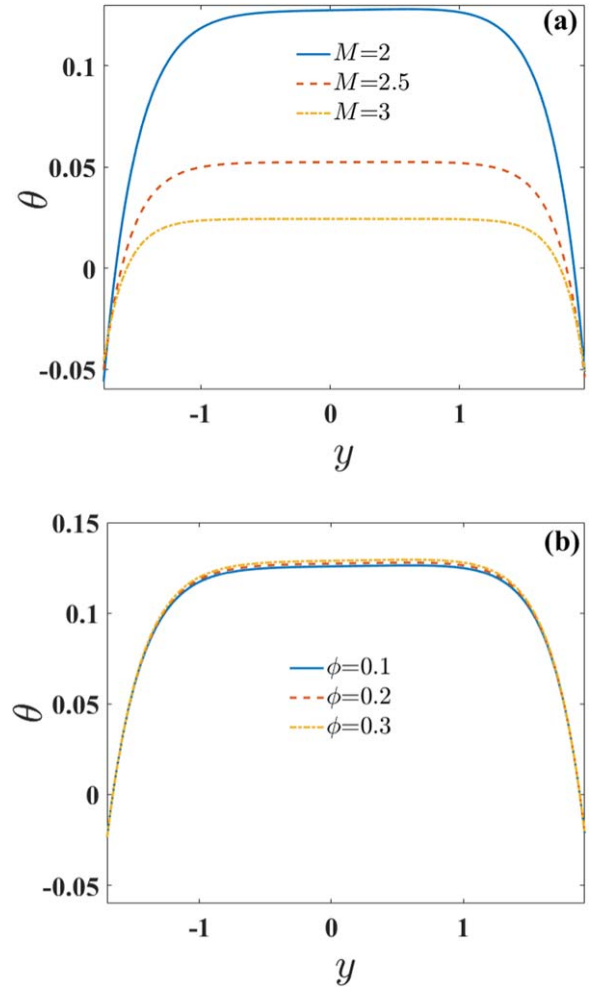


Figure 5. θ versus y for varying (a) M and (b) ϕ .

walls of the channel is given by [2]

$$y = h(x, t) = a + b \sin\left(\frac{2\pi}{\lambda}(x - ct)\right), \quad (1)$$

where c is the wave speed and t is the time.

The equations that govern the flow can be written as follows [14]:

$$\frac{\partial u}{\partial x} + \frac{\partial v}{\partial y} = 0, \quad (2)$$

$$\rho\left(\frac{\partial u}{\partial t} + u\frac{\partial u}{\partial x} + v\frac{\partial u}{\partial y}\right) = -\frac{\partial p}{\partial x} + \frac{\partial \tau_{xx}}{\partial x} + \frac{\partial \tau_{xy}}{\partial y} - \sigma_1 B_0^2 u, \quad (3)$$

$$\rho\left(\frac{\partial v}{\partial t} + u\frac{\partial v}{\partial x} + v\frac{\partial v}{\partial y}\right) = -\frac{\partial p}{\partial y} + \frac{\partial \tau_{xx}}{\partial x} + \frac{\partial \tau_{xy}}{\partial y}, \quad (4)$$

$$\begin{aligned} \rho c_p \left(\frac{\partial T}{\partial t} + u \frac{\partial T}{\partial x} + v \frac{\partial T}{\partial y} \right) &= \frac{\partial}{\partial x} \left(k(T) \frac{\partial T}{\partial x} \right) \\ &+ \frac{\partial}{\partial y} \left(k(T) \frac{\partial T}{\partial y} \right) + \tau_{xx} \frac{\partial u}{\partial x} + \tau_{yy} \frac{\partial v}{\partial y} \\ &+ \tau_{xy} \left(\frac{\partial v}{\partial x} + \frac{\partial u}{\partial y} \right) = 0, \end{aligned} \quad (5)$$

$$\begin{aligned} \frac{\partial C}{\partial t} + u \frac{\partial C}{\partial x} + v \frac{\partial C}{\partial y} &= D_m \left(\frac{\partial^2 C}{\partial x^2} + \frac{\partial^2 C}{\partial y^2} \right) \\ &+ \frac{D_m K_T}{T_m} \left(\frac{\partial^2 T}{\partial x^2} + \frac{\partial^2 T}{\partial y^2} \right). \end{aligned} \quad (6)$$

The above equations represent the continuity, momentum in x and y coordinates, temperature, and concentration equations, respectively.

The flexible wall motions equation is governed by [29, 30]

$$-\tau \frac{\partial^2}{\partial x^2} + n_1 \frac{\partial^2}{\partial t^2} + n_2 \frac{\partial}{\partial t} + n_3 \frac{\partial^4}{\partial x^4} + H = p - p_0. \quad (7)$$

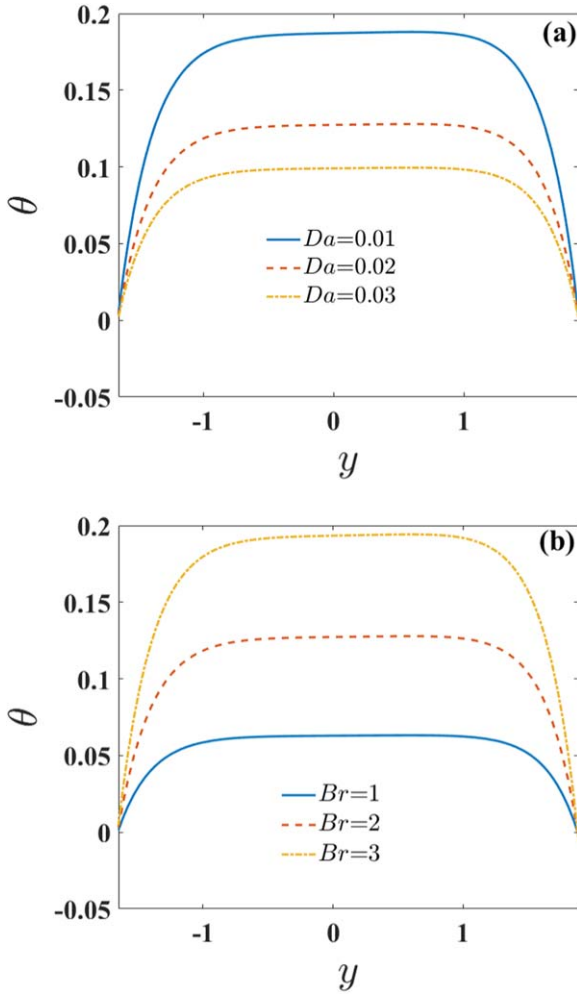


Figure 6. θ versus y for varying (a) Da and (b) Br .

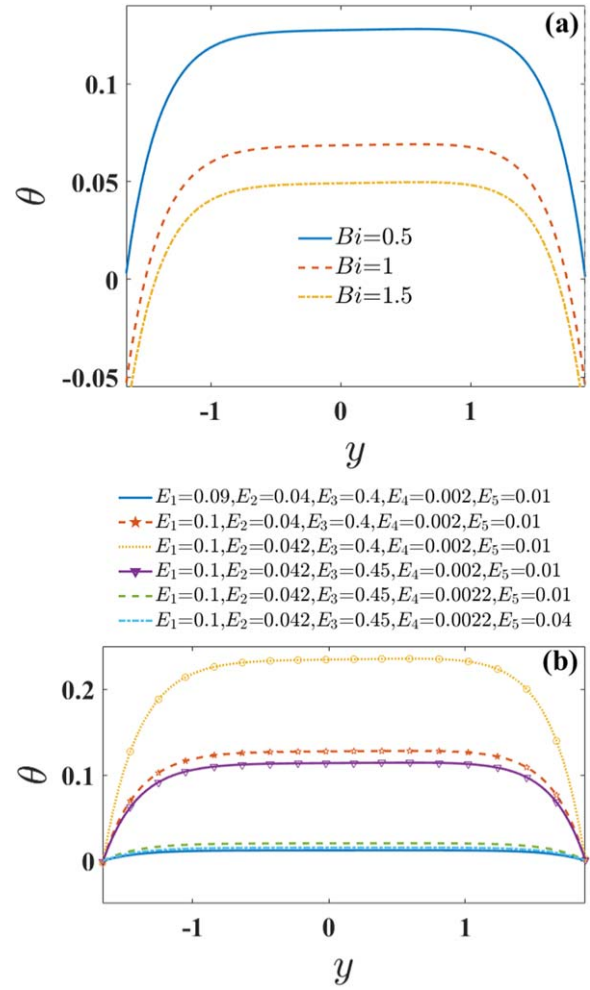


Figure 7. θ versus y for varying (a) Bi and (b) $E_1 - E_5$.

By using the x component of momentum, the continuity of stress at $y = \pm H$ is given by

$$\frac{\partial p}{\partial x} = \frac{\partial \tau_{xx}}{\partial x} + \frac{\partial \tau_{xy}}{\partial y} - \rho \left(\frac{\partial u}{\partial t} + u \frac{\partial u}{\partial x} + v \frac{\partial u}{\partial y} \right) - \sigma_1 B_0^2 u. \tag{8}$$

The non-dimensional quantities of interest are given below

$$x' = \frac{x}{\lambda}, \quad y' = \frac{y}{a}, \quad u' = \frac{u}{c}, \quad v' = \frac{v}{c\xi}, \quad h' = \frac{h}{a}, \quad c_p = \frac{a}{\lambda},$$

$$p' = \frac{pa^2}{\mu\lambda c}, \quad Re = \frac{ac}{\vartheta}, \quad \vartheta = \frac{\mu_0}{\rho}, \quad \tau'_{xx} = \frac{a\tau_{xx}}{\mu c}, \quad \varepsilon = \frac{b}{a},$$

$$t' = \frac{tc}{\lambda}, \quad \tau'_{xy} = \frac{a\tau_{xy}}{\mu c}, \quad \tau'_{yy} = \frac{a\tau_{yy}}{\mu c}, \quad \psi' = \frac{\psi}{ac},$$

$$M = \sqrt{\frac{\sigma_1}{\mu}} B_0 a, \quad E_1 = \frac{-\tau a^3}{\lambda \mu^3 c}, \quad Pr = \frac{\mu c_p}{k_0}, \quad Sc = \frac{\mu}{\rho D_m},$$

$$E_2 = \frac{n_1 ca^3}{\lambda^3 \mu}, \quad E_3 = \frac{n_2 a^3}{\lambda^3 \mu}, \quad E_4 = \frac{n_3 a^3}{\lambda^5 \mu c}, \quad E_5 = \frac{Ha^3}{\lambda \mu c},$$

$$\theta = \frac{T - T_0}{T_0}, \quad Sr = \frac{\rho D_m K_T T_0}{T_m \mu C_0}, \quad Ec = \frac{c^2}{c_p T_0}, \quad \sigma = \frac{C' - C_0}{C_0}. \tag{9}$$

Using equation (9) in the equations (2)–(6) with the assumption of long wavelength and small Reynolds number, the resulting non-dimensional governing equations result in the following form [14]

$$\frac{\partial p}{\partial x} = \frac{\partial \tau_{xy}}{\partial y} - M^2(u + 1), \tag{10}$$

$$\frac{\partial p}{\partial y} = 0, \tag{11}$$

$$\frac{\partial}{\partial y} \left(k(\theta) \frac{\partial \theta}{\partial y} \right) + Br \tau_{xy} \left(\frac{\partial u}{\partial y} \right) = 0, \tag{12}$$

$$\frac{\partial^2 \sigma}{\partial y^2} + Sc Sr \frac{\partial^2 \theta}{\partial y^2} = 0, \tag{13}$$

where τ_{xy} is the constitutive equation of Bingham fluid and it is given by [32]

$$\left. \begin{aligned} \tau_{xy} &= \frac{\partial u}{\partial y} + \tau_0 \quad \text{for } \tau \geq \tau_0 \\ \tau_{xy} &= 0 \quad \text{for } \tau \leq \tau_0 \end{aligned} \right\}, \tag{14}$$

where τ_0 is the yield stress. The corresponding non-dimensional boundary conditions are given by [32]

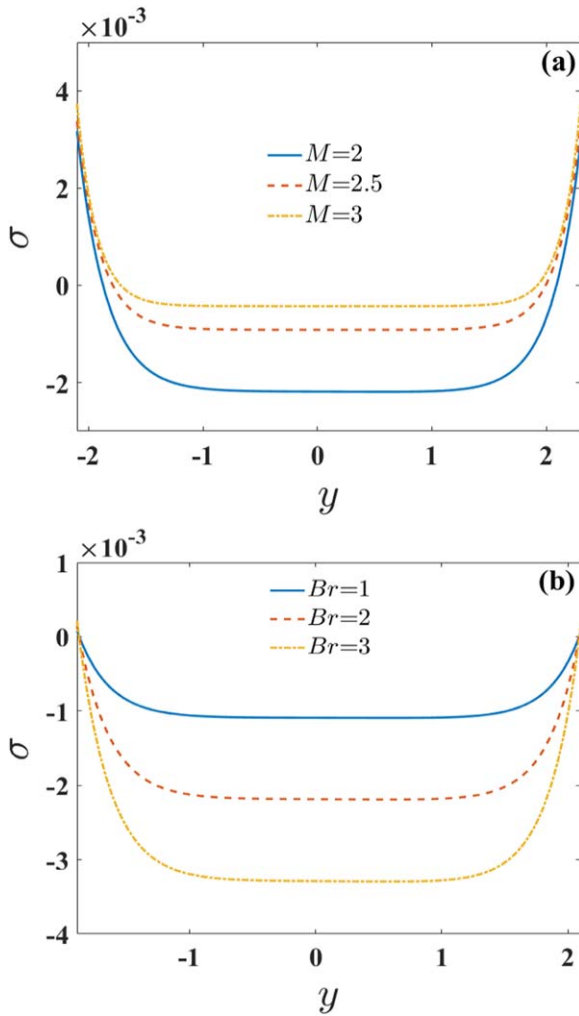


Figure 8. σ versus y for varying (a) M and (b) Br .

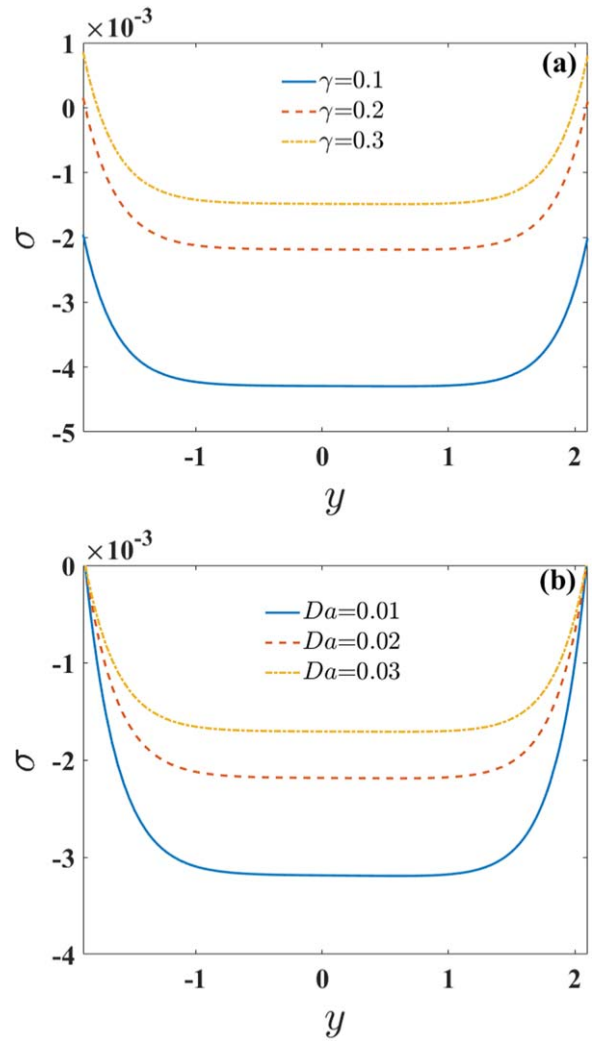


Figure 9. σ versus y for varying (a) γ and (b) Da .

$$\left. \begin{aligned} u + \frac{\sqrt{Da}}{\alpha} \frac{\partial u}{\partial y} &= -1 \\ \frac{\partial \theta}{\partial y} + Bi\theta &= 0 \\ \sigma + \gamma \frac{\partial \sigma}{\partial y} &= 0 \end{aligned} \right\} \text{at } y = h = 1 + \varepsilon \sin [2\pi(x - t)],$$

$$\frac{\partial u}{\partial y} = \tau_0, \quad \frac{\partial \theta}{\partial y} = 0, \quad \frac{\partial \sigma}{\partial y} = 0 \text{ at } y = 0, \tag{16}$$

The thermal conductivity varies with respect to temperature and is defined as below [32]

$$k(\theta) = 1 + \phi \theta, \text{ for } \phi < 1, \tag{17}$$

where ϕ is the coefficient of thermal conductivity.

3. Solution methodology

The velocity expression is obtained by solving equation (10) with the help of boundary conditions (15) and (16)

$$u = \frac{1}{M^2(\alpha \cosh(hM) + \sqrt{Da} M \sinh(hM))} \times \begin{bmatrix} \sqrt{Da} M [M\tau_0 \cosh(M(h - y)) + (M^2 + P)\sinh(hM)] \\ + \alpha M\tau_0 \sinh(M(h - y)) - \alpha(M^2 + P)\cosh(hM) \\ - \alpha P \cosh(My) \end{bmatrix} \tag{18}$$

On utilizing the boundary condition $u' = 0$ at $y = y_0$ the plug flow region is given by

$$\tau_0 = - \frac{\alpha P \sinh(My_0)}{M[\alpha \cosh(M(h - y_0)) + \sqrt{Da} M \sinh(M(h - y_0))]} \tag{19}$$

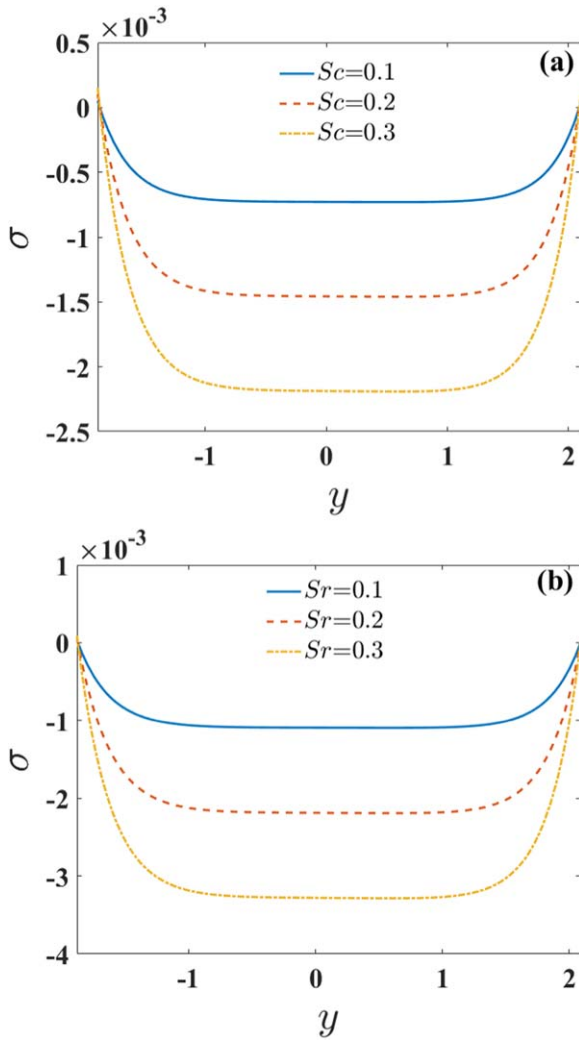


Figure 10. σ versus y for varying (a) Sc and (b) Sr .

Noting here that the x -component of the pressure gradient P appearing in equation (18) and defined by equation (8) is simplified as follows

$$P = 8\varepsilon\pi^3 \left(\frac{E_3}{2\pi} \sin 2\pi(x - t) - \left[E_1 + E_2 - 4\pi^2 E_4 - \frac{E_5}{4\pi^2} \right] \times \cos 2\pi(x - t) \right) \quad (20)$$

The stream function can be found by integrating equation (18) with the condition $\psi = 0$ at $y = 0$.

Because of the nonlinearity in the equation (12), we cannot find an exact solution to the problem. We therefore embrace the perturbation technique to extend the temperature range θ to tiny amount of variable thermal conductivity ϕ as follows

$$\theta = \theta_0 + \phi\theta_1 + O(\phi^2). \quad (21)$$

Substitute the equation (21) to the equation (12) and by applying the boundary conditions (15) and (16), we acquire the temperature expression. Further, the expression for concentration is achieved by making use of the temperature equation.

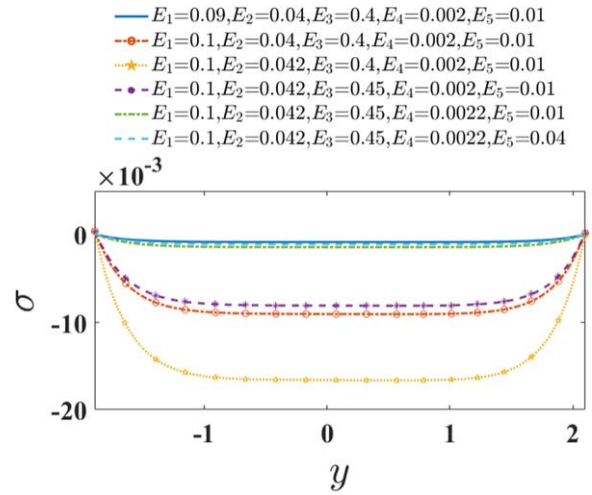


Figure 11. σ versus y for varying $E_1 - E_5$.

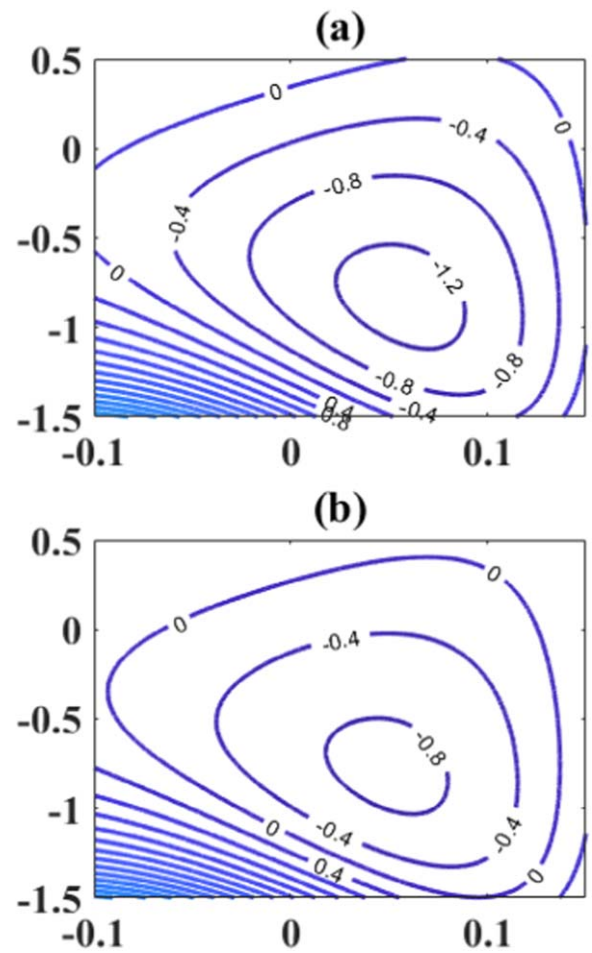


Figure 12. Streamlines for varying magnetic parameter when (a) $M = 1$ and (b) $M = 2$ (with x -axis horizontal, y -axis vertical).

4. Validation of the model

In comparison, it can be noticed that the inclusion of a porous parameter enhances the velocity profile (see figure 2). In the absence of porous parameter and yield stress, the velocity expression obtained in equation (18) reduces to the special

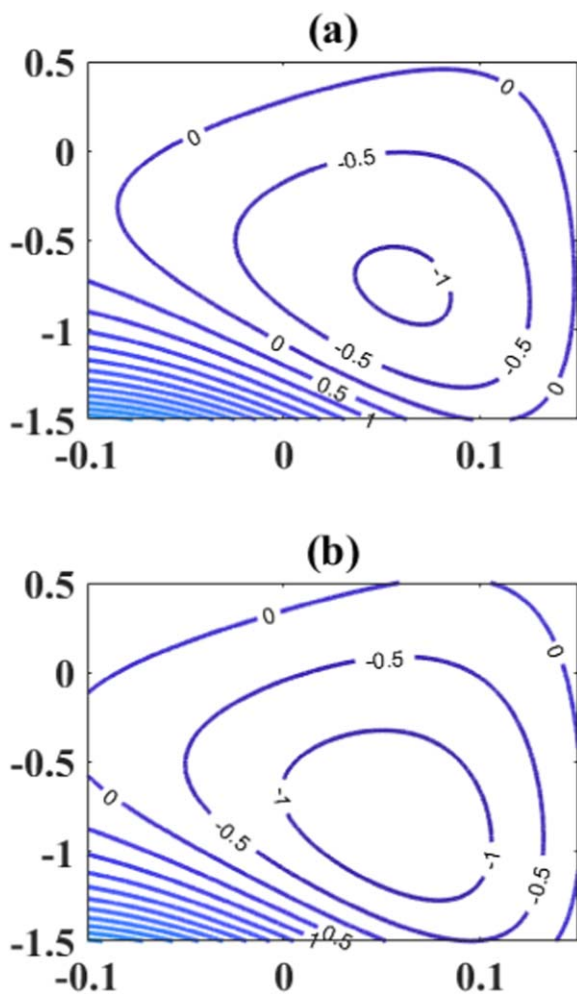


Figure 13. Streamlines for varying porous parameter when (a) $Da = 0.01$ and (b) $Da = 0.02$ (with x -axis horizontal, y -axis vertical).

case ($\alpha = 0$, $\alpha_1 = 0$ and $\lambda_1 = 0$) of Manjunatha et al [33]. Further, the behavior of velocity, temperature, and concentration profiles are in concurrence with the results of Hayat et al [35].

5. Results and discussions

In this section, the impacts of M , Da , ϕ , α , γ , Br , Bi , Sc , Sr , E_1 , E_2 , E_3 , E_4 and E_5 on velocity (u), temperature (θ), concentration (σ) and streamlines (ψ) are analyzed and discussed through graphs 3–15. Further, the MATLAB software has been utilized for the pictorial representations of relevant parameters of interest on physiological quantities with the fixed values of $E_1 = 0.1$, $E_2 = 0.04$, $E_3 = 0.4$, $E_4 = 0.002$, $E_5 = 0.01$, $t = 0.1$, $x = 0.2$, $\varepsilon = 0.6$, $M = 1$, $\alpha = 0.2$, $Sr = 0.3$, $\beta = 0.2$, $\gamma = 0.2$, $Br = 2$, $Sc = 0.2$, $\tau_0 = 0.002$, $\alpha_1 = 0.02$ and $\phi = 0.02$.

Figures 3 and 4 depict the variation of M , Da , α , E_1 , E_2 , E_3 , E_4 and E_5 on velocity profiles. It is apparent from these figures that maximum velocity happens in the center region arising in a parabolic trajectory. Figure 3(a) shows the

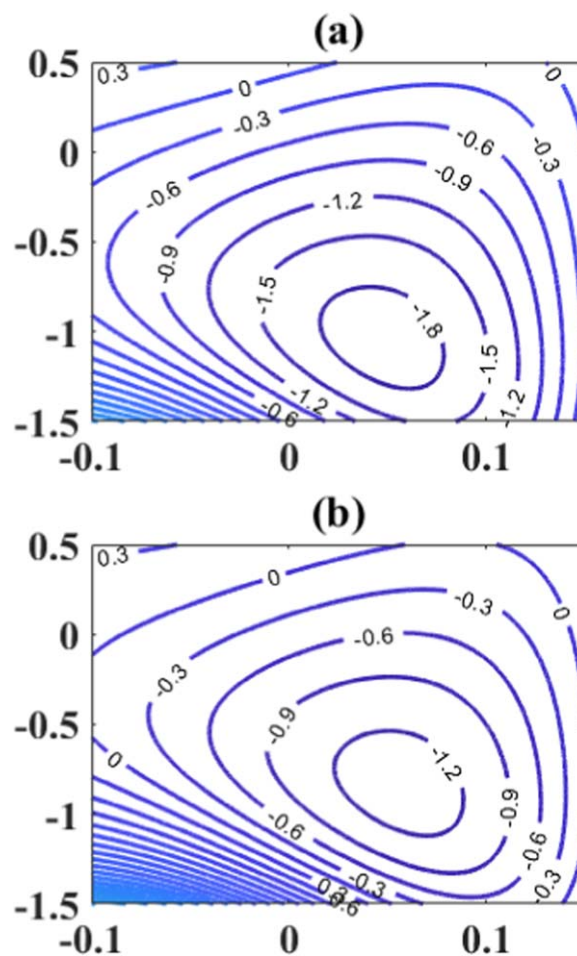


Figure 14. Streamlines for varying velocity slip parameter when (a) $\alpha = 0.1$ and (b) $\alpha = 0.2$ (with x -axis horizontal, y -axis vertical).

impact of the magnetic parameter on the velocity profiles. The figure shows that an increase in the value of magnetic parameter decreases the velocity profile. This conduct is undeniable as the transverse magnetic field resists the flow. Particularly in blood flow, the transverse magnetic field results in the formation of rouleaux leading to a decrease in the velocity profiles. In the study of blood flow through vessels, consideration of a porous wall is essential. As wall porosity rises, the flow resistance diminishes and thus, fluid velocity near the walls increases (figure 3(b)). Further, the velocity slip parameter is a decreasing function of velocity (figure 4(a)). Figure 4(b) portrays the variation of wall properties on the velocity field. Here, fluid flows rapidly with E_1 and E_2 and the flow is retarded for an increment in the values of E_3 , E_4 and E_5 .

The variations of M , ϕ , Da , Br , Bi , E_1 , E_2 , E_3 , E_4 and E_5 on temperature are scrutinized in figures 5–7. The temperature of fluid rises in the core region resulting in a parabolic trajectory. The effect of viscous dissipation on heat models can contemplate this nature of the graph. Due to the conversion of kinetic energy into inner thermal energy using fluid viscosity, viscous dissipation happens. The effects of magnetic parameter and variable thermal conductivity on the temperature models is shown in figure 5. Figure 5(a) shows

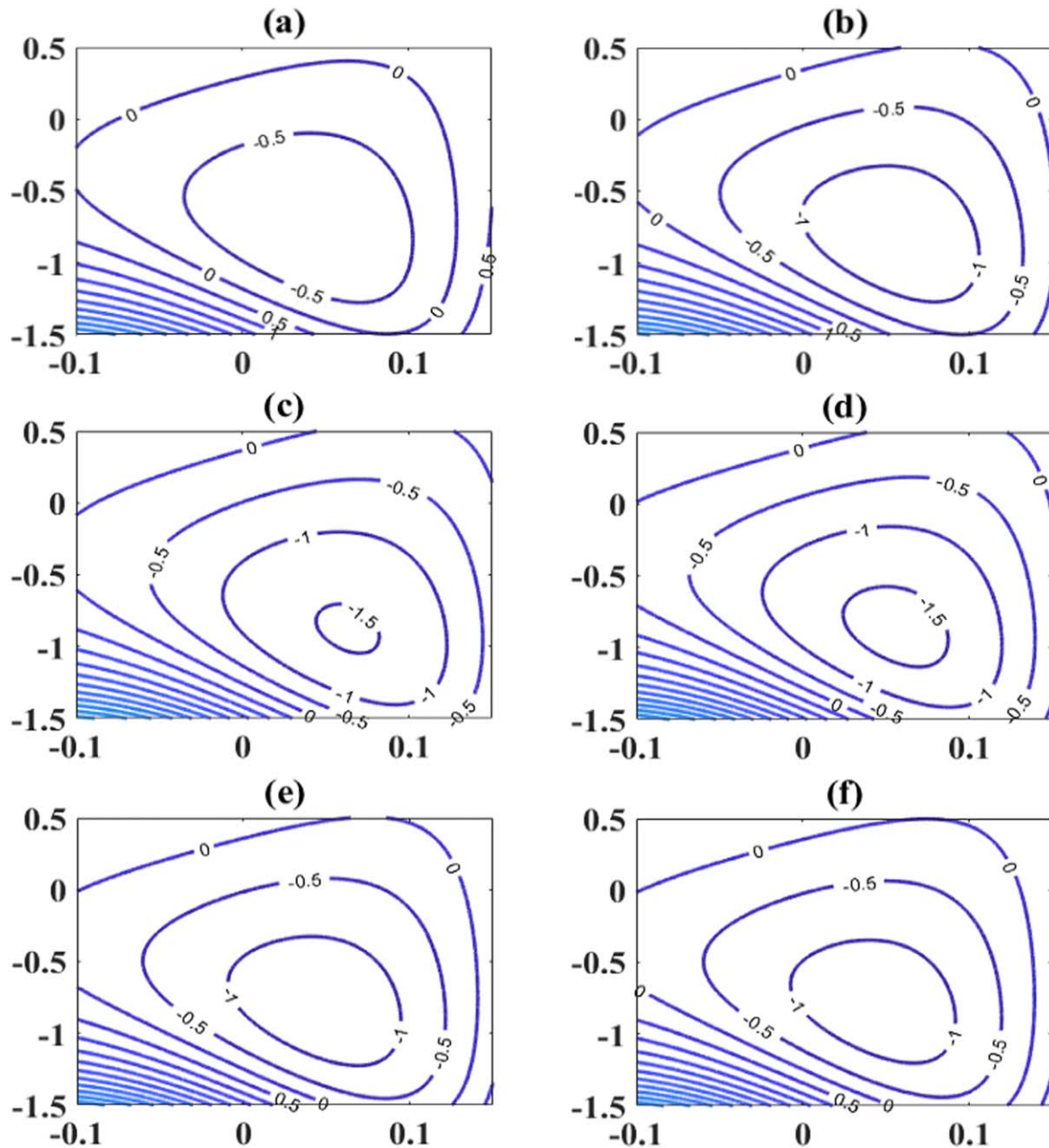


Figure 15. Streamlines with x -axis horizontal and y -axis vertical for varying elastic parameters ($E_1 - E_5$) when (a) $E_1 = 0.09, E_2 = 0.04, E_3 = 0.4, E_4 = 0.002, E_5 = 0.01$ (b) $E_1 = 0.1, E_2 = 0.04, E_3 = 0.4, E_4 = 0.002, E_5 = 0.01$ (c) $E_1 = 0.1, E_2 = 0.042, E_3 = 0.4, E_4 = 0.002, E_5 = 0.01$ (d) $E_1 = 0.1, E_2 = 0.042, E_3 = 0.45, E_4 = 0.002, E_5 = 0.01$ (e) $E_1 = 0.1, E_2 = 0.042, E_3 = 0.45, E_4 = 0.0022, E_5 = 0.01$ (f) $E_1 = 0.1, E_2 = 0.042, E_3 = 0.45, E_4 = 0.0022, E_5 = 0.4$.

the magnetic parameter’s declining impact on temperature models. In addition, the higher thermal conductivity increases the temperature of the liquid (see figure 5(b)). This is because the fluids thermal conductivity provides the measurement of the liquid’s capacity to maintain or release the heat in its environment. Thus, when the fluids thermal conductivity within the channel is higher than the temperature of the wall, the thermal value of the liquid increases. Figure 6 displays the variation in the temperature profiles for an increment in the value of a porous parameter and Brinkmann number. The declining effect on temperature profiles is noticed for an increase in the value of porous parameter figure 6(a). For an

increase in the Brinkmann number, the reverse conduct is observed (figure 6(b)). This is ascribed to fluid strength intensification owing to an increase in the Brinkmann number significance, which triggers the impacts of viscous dissipation to inflate the inner thermal energy. The impacts of Biot number and wall properties on the temperature profiles have been shown in figure 7. Here, a drop in the temperature is observed for an increase in the value of the Biot number. This is because an increase in the magnitude of Biot number leads to a decrease in thermal conductivity of the fluid, which in turn reduces the temperature (figure 7(a)). From figure 7(b), the temperature profiles enhance for increasing values of

E_1 and E_2 , whereas an opposite tendency is noticed for E_3 , E_4 and E_5 .

In comparison with the temperature profiles, the concentration profiles show the opposite behavior. This is physically logical because heat and mass are recognized to be reverse. Besides, the patterns indicate that the fluid particles are more concentrated near the walls of the channel. This conduct is biologically evident as the main sugar components and other liquids spread into the neighboring neurons and organs. Figure 8 is graphed to highlight the effects of the magnetic parameter and Brinkmann number on the concentration profiles. From the figure, it observed that larger values of magnetic parameter enhance the concentration profiles (figure 8(a)), whereas the concentration profiles diminish with an increase in the amount of Brinkmann number (figure 8(b)). Figure 9 is graphed to show the effects of concentration slip and porous parameter on the concentration profiles. From the figure, an increase in the value of a slip and porous parameter enhances the concentration profiles. Further, the impact of Schmidt and Soret numbers show the opposite behavior as that of concentration slip parameter (see figure 10). Figure 11 shows the variation of wall properties on the concentration profiles. It is clearly seen that the flow is retarded for increasing values of E_1 and E_2 and the opposite behavior is noticed for E_3 , E_4 and E_5 .

Trapping is an extraordinary phenomenon in understanding the biological liquid flux characteristics such as thrombus movement in blood vessels and the motion of chyme through the gastrointestinal tract. The peristaltic system in these schemes enables us to understand the development of the bolus. It is discovered that the quantity of the trapped bolus is a decreasing function of the magnetic parameter (see figure 12).

The impact of the porous parameter enhances the size of the trapped bolus (figure 13). Further, velocity slip parameter shows the reverse trend as that of variable viscosity (figure 14). Figure 15 shows the impact of wall properties on the trapped bolus. Here, a rise in the values of E_1 , E_2 and E_3 enhances the size of a trapped bolus, whereas the contrary behavior is noticed for E_4 and E_5 .

6. Conclusions

This paper inspects the impact of variable thermal conductivity on the MHD peristaltic flow. The heat and mass transfer characteristics are explored under the effects of convective and wall properties through a uniform porous channel. The essential results of this paper can be summarized as:

- Magnetic parameter decreases velocity and temperature profiles.
- Wall tension and mass characterization parameter enhances the velocity and temperature distribution.
- The temperature profile is a decreasing function of the Biot number.


- The temperature profile increases with an increase in the value of variable thermal conductivity.
- The Soret and Schmidt numbers cause a drop in the concentration profiles.
- The number of bolus formation decreases with an increase in the value of magnetic and velocity slip parameters.

Acknowledgments

The authors would like to thank the reviewers for the constructive and helpful comments that have led to a substantial improvement in the paper.

ORCID iDs

H Vaidya  <https://orcid.org/0000-0001-5343-8039>

C Rajashekhar  <https://orcid.org/0000-0001-8950-7104>

References

- [1] Latham T W 1966 Fluid motion in a peristaltic pump *MS Thesis* Massachusetts Institute of Technology (Cambridge, USA)
- [2] Raju K K and Devanathan R 1972 Peristaltic motion of a non-Newtonian fluid *Rheological Acta* **111** 70
- [3] Srivastava L M and Srivastava V P 1982 Peristaltic transport of blood: Casson model: II *J. Biomech.* **17** 821
- [4] Kwang-Hua W C 2002 Peristaltic transport within a micro-tube *Phys. Scr.* **65** 283
- [5] Vajravelu K, Sreenadh S and Babu V R 2005 Peristaltic pumping of a Herschel–Bulkley fluid in a channel *Appl. Math. Comput.* **169** 726
- [6] El-Shehawey F and Husseny S Z A 2000 Effect of porous boundaries on peristaltic transport through a porous medium *Acta Mech.* **143** 165
- [7] Khan A A, Ellahi R and Usman M 2013 The effects of variable viscosity on the peristaltic flow of non-Newtonian fluid through a porous medium in an inclined channel with slip boundary conditions *J. Porous Media* **16** 59
- [8] Alsaedi A, Ali N, Tripathi D and Hayat T 2014 Peristaltic flow of couple stress fluid through uniform porous medium *Appl. Math. Mech.* **35** 469
- [9] Latha R, Kumar B R and Makinde O D 2018 Effects of heat dissipation on the peristaltic flow of Jeffery and Newtonian fluid through an asymmetric channel with porous medium *Defect Diffusive Forum* **387** 218
- [10] Manjunatha G and Rajashekhar C 2018 Slip effects on peristaltic transport of Casson fluid in an inclined elastic tube with porous walls *J. Adv. Res. Fluid Mech. Therm. Sci.* **43** 67
- [11] Vaidya H, Rajashekhar C, Manjunatha G and Prasad K V 2019 Effect of variable liquid properties on peristaltic flow of Rabinowitsch fluid in an inclined convective porous channel *Eur. Phys. J. Plus* **134** 231
- [12] Vaidya H, Rajashekhar C, Manjunatha G and Prasad K V 2019 Peristaltic mechanism of a Rabinowitsch fluid in an inclined channel with compliant wall and variable liquid properties *J. Braz. Soc. Mech. Sci. Eng.* **4** 52

- [13] Ellahi R, Bhatti M M and Vafai K 2014 Effects of heat and mass transfer in peristaltic flow in a non-uniform rectangular duct *Int. J. Heat Mass Transfer* **19** 706
- [14] Ramesh K 2016 Influence of heat and mass transfer on peristaltic flow of a couple stress fluid through porous medium in the presence of inclined magnetic field in an inclined asymmetric channel *J. Mol. Liq.* **219** 256
- [15] Bhatti M M and Zeeshan A 2016 Heat and mass transfer analysis on peristaltic flow of particle-fluid suspension with slip effects *J. Mech. Med. Biol.* **17** 1750028
- [16] Samreen S, Hina S, Akbar N S and Mir N A 2019 Heat and peristaltic propagation of water-based nanoparticles with variable fluid features *Phys. Scr.* **94** 125704
- [17] Abbasi F M, Shanakhat I and Shehzad S A 2019 Analysis of entropy generation in peristaltic nanofluid flow with Ohmic heating and Hall current *Phys. Scr.* **94** 025001
- [18] Nakhchi M E, Nobari M R H and Tabrizi H B 2012 Non-similarity thermal boundary layer flow over a stretching flat plate *Chin. Phys. Lett.* **29** 104703
- [19] Nakhchi M E and Esfahani J A 2019 Numerical investigation of turbulent Cu-water nanofluid in heat exchanger tube equipped with perforated conical rings *Adv. Powder Technol.* **30** 1338
- [20] Nakhchi M E and Esfahani J A 2019 Numerical investigation of different geometrical parameters of perforated conical rings on flow structure and heat transfer in heat exchangers *Appl. Therm. Eng.* **156** 494
- [21] Borujerdi N A and Nakhchi M E 2019 Prediction of local shear stress and heat transfer between internal rotating cylinder and longitudinal cavities on stationary cylinder with various shapes *Int. J. Therm. Sci.* **138** 512
- [22] Nakhchi M E and Esfahani J A 2020 Numerical investigation of heat transfer enhancement inside heat exchanger tubes fitted with perforated hollow cylinders *Int. J. Therm. Sci.* **147** 106153
- [23] El-Shehawey E-S F and El-Sebaei W 2001 Couple-stress in peristaltic transport of a magneto-fluid *Phys. Scr.* **64** 401
- [24] Mishra J C and Shit G C 2007 Effect of magnetic field on blood flow through an artery: a numerical model *Comput. Technol.* **12** 3
- [25] Sinha A, Shit G C and Ranjit N K 2015 Peristaltic transport of MHD flow and heat transfer in an asymmetric channel: effects of variable viscosity, velocity-slip and temperature jump *Alexandria Eng. J.* **54** 691
- [26] Oudina F M and Makinde O D 2018 Numerical simulation of oscillatory MHD natural convection in cylindrical annulus: prandtl number effect *Defect Diffus. Forum* **387** 417
- [27] Guo X, Zhou J, Xie H and Jiang Z 2018 MHD peristaltic flow of fractional Jeffrey model through porous medium *Mech. Problems Eng.* **2018** 10
- [28] Hatyat T, Zahir H, Tanveer A and Alsaedi A 2018 Soret and Dufour effects on MHD peristaltic flow of Prandtl fluid in a rotating channel *Results Phys.* **8** 1291
- [29] Hayat T, Javed M and Ali N 2008 MHD peristaltic of a Jeffrey fluid in a channel with compliant walls and porous space *Transp. Porous Media* **74** 259
- [30] Srinivas S, Gayathri R and Kothandapani M 2009 The influence of slip conditions, wall properties and heat transfer on MHD peristaltic transport *Comput. Phys. Commun.* **180** 2115
- [31] Javed M, Hayat T and Alsaedi A 2014 Peristaltic flow of Burgers' fluid with compliant walls and heat transfer *Appl. Math. Comput.* **244** 654
- [32] Manjunatha G, Rajashekhar C, Vaidya H, Prasad K V and Vajravelu K 2019 Impact of heat and mass transfer on the peristaltic mechanism of Jeffrey fluid in a non-uniform porous channel with variable viscosity and thermal conductivity *J. Therm. Anal. Calorim.* **139** 1213
- [33] Manjunatha G, Rajashekhar C, Vaidya H, Prasad K V, Makinde O D and Viharika J U 2019 Impact of variable transport properties and slip effects on MHD Jeffrey fluid flow through channel *Arab. J. Sci. Eng.* **45** 417
- [34] Akram S, Nadeem S and Hussain A 2014 Effects of heat and mass transfer on peristaltic flow of a Bingham fluid in the presence of inclined magnetic field and channel with different wave forms *J. Magn. Magn. Mater.* **362** 184
- [35] Hayat T, Farooq S, Mustafa M and Ahmad B 2017 Peristaltic transport of Bingham plastic fluid considering magnetic field, Soret and Dufour effects *Results Phys.* **7** 2000
- [36] Manjunatha G, Rajashekhar C, Vaidya H and Prasad K V 2019 Peristaltic mechanism of Bingham liquid in a convectively heated porous tube in the presence of variable liquid properties *Spec. Top. Rev. Porous Media-Int. J.* **10** 187